

C,N and key heavy elements in metal-poor and very metal-poor carbon-enhanced stars

T. Masseron¹, B. Plez¹, F. Primas², S. Van Eck³ and A. Jorissen³

¹GRAAL, Université Montpellier II, 34095 Montpellier cedex 5, France

email: masseron@graal.univ-montp2.fr

²European Southern Observatory (ESO), Karl-Schwarzschild-Str. 2, 85749 Garching b. München, Germany

³Institut d'Astronomie et d'Astrophysique, Université Libre de Bruxelles, CP 226, Boulevard du Triomphe, 1050 Bruxelles, Belgium

Abstract. A new class of carbon-rich stars was revealed by large surveys of very metal-poor objects, the carbon-enhanced metal-poor stars (CEMPs). This carbon enhancement is reminiscent of that found in classical CH stars, which despite being halo stars, are not as metal-poor as CEMPs. Although a mass-transfer scenario similar to that formerly at work in CH stars could account for the abundance pattern of CEMPs, differences arise for some key heavy elements. Moreover, statistical studies find 14% of metal-poor C-rich stars among very metal-poor stars. Thus, this important population of stars represents a precious testimony for nucleosynthesis and chemical evolution at early stages of the Galaxy. We have started a detailed analysis of a large sample of both CH and metal-poor C-rich stars. Here we present results concerning the chemical composition obtained via high resolution and high signal-to-noise VLT-UVES spectra, with special emphasis on the challenges encountered during the abundance analysis. The discussion also includes preliminary results of our ongoing radial velocity monitoring programme which aims at evaluating the relevance of the binary scenario.

Keywords. Stars: carbon stars: Population II stars: abundances

1. Introduction

A subgroup of carbon stars, the so-called CH stars, were first distinguished from other carbon stars some 60 years ago (Keenan 1942). Their chief characteristics were defined as follows: strong CH absorption lines, strong Swan bands of C₂, strong resonance lines of Ba II and Sr II (later shown to reflect genuine overabundances of s-process elements), weak lines of the iron-group elements and large radial velocities.

The enigmatic nature of CH stars arises from the fact that like the barium and R stars with which they share similar luminosities and carbon overabundances (Scalo 1976), CH stars are not luminous enough to be on the asymptotic giant branch (AGB), as required by their s-process overabundances. Since it was discovered that all CH stars in the field were spectroscopic binaries (McClure & Woodsworth 1990), the binary scenario appeared as a very natural explanation: CH stars have been polluted by their companion, formerly on the AGB, now a defunct white dwarf.

During the 90s, extensive surveys of metal-deficient stars have been carried out (e.g. the HK survey of Beers *et al.* 1992; the Hamburg/ESO survey, Wisotzki *et al.* 1996) in order to identify the oldest stellar populations in the Galaxy. One of the most exciting findings of these surveys is the large fraction (14% in the metallicity range $[\text{Fe}/\text{H}] \leq -2.5$ compared to 1–2 % among stars of higher metal abundances) of very metal-poor stars

exhibiting anomalously strong CH-bands, resembling their more metal-rich counterparts, the CH-stars. However, the analogy has still to be proven and some recent results have cast doubts on the mass transfer scenario, which is the accepted explanation for the origin of the classical CH stars. Conflicting evidences include the absence of radial-velocity variations over eight years for three carbon enhanced metal-poor stars (CEMP) subgiants (Preston & Sneden, 2001), and the discovery of carbon- but not s-process-enhanced stars (e.g. Sneden *et al.* 1996).

Because of these puzzling characteristics, this emergent class of stars offers a very good field of investigation to probe the early stages of Galactic and stellar evolution.

2. Observations

Our chemical analysis is based on high-resolution and high signal-to-noise VLT/UVES spectra of 21 targets which were originally observed to extend the work of Van Eck *et al.* (2001) on lead stars. Our radial velocity monitoring programme is based instead on high resolution but lower signal-to-noise spectra. The detected binaries from this survey and from the literature are denoted by red circled points in figures 3, 5 and 6.

The challenging analysis of our diverse sample, including dwarfs, subgiants and giants, covering the spectral types from F5 to K8, and metallicities between -3.6 and $+0.2$, requires to carefully derive abundances from spectra crowded by carbon molecular lines, characteristic of this category of stars.

3. Abundance analysis

All our abundances are derived by comparing the observed spectra with synthetic ones, computed with the “turbospectrum” package, a program adapted for cool stars and developed by B. Plez (Alvarez & Plez 1998). This program uses OSMARCS atmosphere models, initially developed by Gustafsson *et al.* (1975) and later improved by Plez *et al.* (1992); see Gustafsson *et al.* (2003) for details on recent improvements.

Effective temperatures have been derived from photometry available in the literature, using the calibration of Alonso *et al.* (1999). They were cross-checked by forcing the abundance determined from individual Fe I lines to show no dependence on excitation potential. The gravity was constrained by imposing the ionisation equilibrium of Fe I and Fe II. The microturbulent velocity was set by requiring no trend of Fe I abundance with reduced equivalent widths.

We have assembled an accurate line list for Mg, Ba, Eu and Pb including their hyperfine structure and their respective isotopic shifts. C abundance and its isotopic ratio, as well as N abundance, are deduced from CN and CH molecular lines (cf. Hill *et al.* 2002).

Carbon and nitrogen molecules can have a deep impact on the thermal structure of models as shown in figure 1. This diagram shows the comparison between a “standard”, i.e. solar-scaled metallicity model, and a C- and N-enhanced model. Using a standard metal-poor model, differences in the derived abundances can reach up to 1.5 dex for models at $T_{\text{eff}} \approx 4500\text{K}$ (whereas at higher effective temperature, e.g. 6000K, errors are negligible). Based on the extensive tests we have carried out, similar discrepancies are found also at other metallicities and gravities. These figures stress the necessity of using, especially for cool stars, specifically tailored model atmospheres with the corresponding C, N, O overabundances.

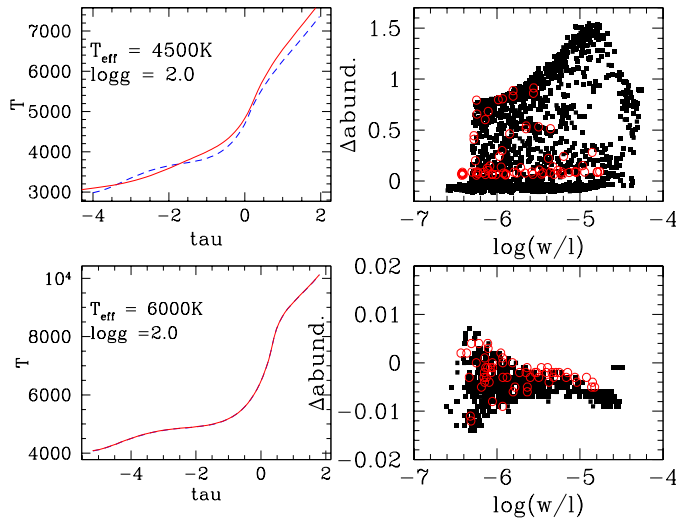


Figure 1. left panels: Comparison of a metal-poor model ($[Fe/H] = -3.0$) with all abundances scaled down (dashed blue line) with C- and N-enhanced ($[C/Fe] = +2.0$, $[N/Fe] = +2.0$) models (solid red line). right panels: Errors on Fe abundances when using a non specific tailored model for C-rich stars. Open circles represent singly ionised Fe lines and black squares neutral Fe lines. upper panels: $T_{\text{eff}} = 4500\text{K}$, $\log g = 2.0$ lower panels: $T_{\text{eff}} = 6000\text{K}$, $\log g = 2.0$

4. Results

4.1. Light elements

Figure 2 presents an almost exhaustive compilation of carbon abundances from the literature, obtained from spectral syntheses. While the bulk of the stars are non C-rich, the family of C-rich stars is clearly distinguishable, especially at low $[Fe/H]$. By inspecting this figure, there may be a hint that C enhancement in C-rich stars increases with decreasing metallicity. Even the lowest metallicity stars HE 0107-5240 ($[Fe/H] = -5.3$, Christlieb *et al.* 2002) and HE1327-2326 ($[Fe/H] = -5.4$, Frebel *et al.* 2005) follow this trend and show carbon abundances only a factor of 30 down from the solar value. This could suggest that the C abundance in such objects is primary, coming from He-burning. But the question is whether the carbon is intrinsic or extrinsic. Our radial velocity monitoring complemented

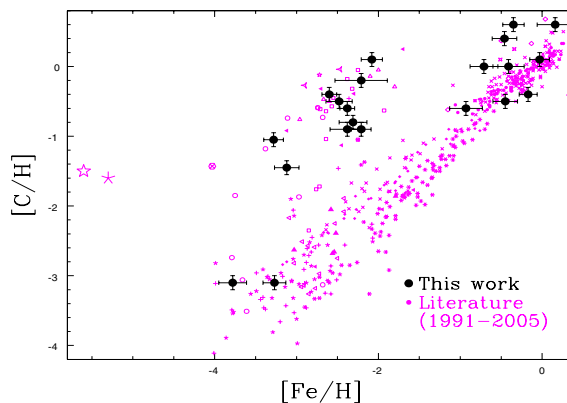


Figure 2. Carbon-enhanced stars compared to “normal” stars.

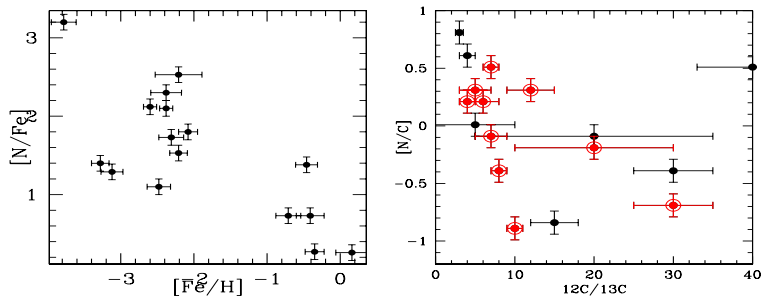


Figure 3. Detected binaries are red circled. (a) N enhancement at low metallicity, but large scatter. (b) Signature of destruction of ^{12}C with production of N during CN burning.

with literature data revealed that 59% (or 10/17) of our sample stars show variations in their radial velocity at the 3σ (where $\sigma = 1\text{km/s}$) level with 3 measurements over about 2 years. This percentage is compatible with the percentage of McClure & Woodworth (1990) and Lucatello *et al.* (2005) detected binaries, who deduced that all these stars are in binary systems. Furthermore, their non C-rich counterparts of the same metallicity (Spite *et al.* 2005), which do not have a binarity rate as high as the C-rich stars, do not show such an amount of carbon ($[C/Fe] < 0.5$). This confirms that carbon comes from a now extinct companion and validates the mass-transfer scenario. Note that some of our targets at low-metallicity do not appear to be C-rich. These targets have been removed from figures 3, 4, 5 and 6. All our targets were pre-selected to be C-enhanced from the HK (Beers *et al.* 1992) and the HES (Wisotzki *et al.* 1996) surveys, and belong to the subset of 14% of CEMP stars among metal-poor stars. The presence of two non-CEMP stars unraveled by the present detailed abundance study among a sample of 12 stars indicates that this 14% frequency must probably be revised downwards (see also Cohen *et al.* 2005, this volume).

Figures 3 and 4 present the abundances we have derived for C, N, $^{12}C/^{13}C$ and Mg. The figure 3a show that C-rich stars can also be N-rich. The $^{12}C/^{13}C$ ratio is generally low, often close to the CN-cycle equilibrium value (figure 3b). Note the anti-correlation between the N overabundance and $^{12}C/^{13}C$, characteristic of the operation of the CN cycle. The stars of our sample with low $^{12}C/^{13}C$, and still on the main sequence, are binaries, supporting the mass-transfer scenario.

The general trend in figure 4 between $[Mg/Fe]$ and metallicity is similar to that observed in non C-rich stars (see Cayrel *et al.* 2004). The scatter is larger however and may reflect processes occurring in intermediate-mass stars during their AGB phase, like the hot-bottom burning or the operation of $^{22}Ne(\alpha, n)^{25}Mg$.

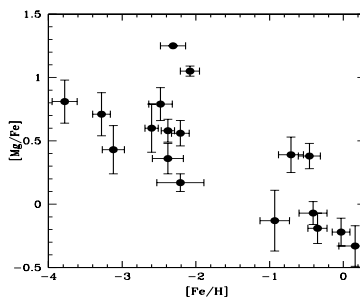


Figure 4. Mg trend similar to non C-rich stars, except for a somewhat larger scatter.

4.2. Heavy elements

Solar Ba is synthesized mainly by s-process whereas Eu is formed via r-process (see, however, Goriely 2005, this volume). s-process elements are produced in AGBs, and r-process elements originate from supernovae.

Thus the [Ba/Eu] ratio, as shown in figure 5, can be used as a diagnostic of the origin of heavy elements in stars. On this plot, most of the C-rich stars lie around the solar s-process limit (dashed line), confirming that C, N and neutron-capture elements present in these stars have certainly been synthesized by AGB stars. According to calculations

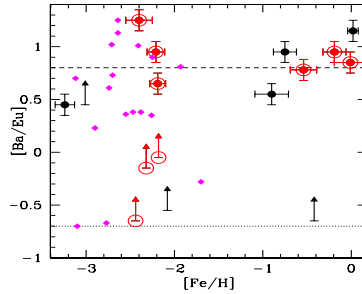


Figure 5. Magenta diamonds from literature. The upper dashed line represents solar s-process and the lower dotted line solar r-process (Arlandini *et al.* 1999).

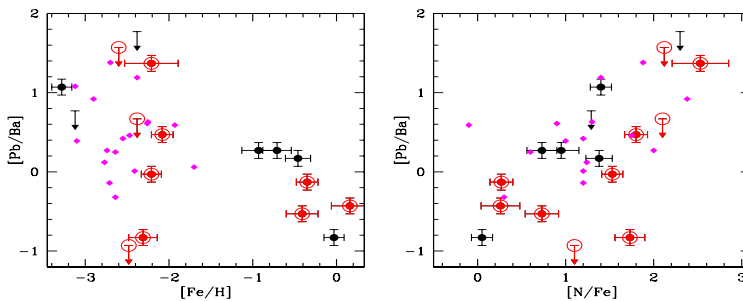


Figure 6. Same symbols as figure 5. (a) The largest [Pb/Ba] ratios are indeed found at the lowest metallicities, as expected, but the scatter is much larger than predicted by the standard models for the operation of the s-process in AGB stars. (b) However, the scatter of N at low metallicity of figure 3a cancels for the scatter of [Pb/Ba] at low metallicity (from Lucatello, 2003)

by Goriely & Mowlavi (2001), Siess & Goriely (2001) and Busso *et al.* (2001), the s-process is quite efficient at low metallicities (because of the smaller relative number of Fe seed nuclei; Clayton 1988) so as to produce elements up to the third s-process peak involving Pb and Bi. In figure 6a, the largest [Pb/Ba] ratios are indeed found at the lowest metallicities, as expected, but the scatter is much larger than predicted by the standard models for the operation of the s-process in AGB stars. However, the clear correlation in figure 6b indicates that a common mechanism or the same physical conditions must drive N production and s-process. N is believed to be produced by hot bottom burning at the base of the convective zone. Neutron-capture elements are synthesized in the ^{13}C pocket in the He burning shell, and brought to the surface after the third dredge-up (DUP). But HBB and 3^{rd} DUP occur only at high temperatures ($>8.10^7\text{K}$). As mentioned by Goriely & Siess (2001), at low metallicity, low-mass stars can also experience thermal

pulses and third dredge up, because of higher temperatures below the convective zone. This complex interplay between metallicity and mass can be at the origin of the different s-process distributions and different N production levels as observed.

5. Conclusions

The study of C-rich stars gives the opportunity to understand low- and intermediate-mass stars at the early stages of the Galaxy. Their first imprints are the large overabundance of C on their less evolved companion. However, among this distinguishable class, various abundance patterns exist. First of all, a spread of N abundances is observed, but the correlation with $^{12}\text{C}/^{13}\text{C}$ shows that HBB occurred in some C-rich stars and might be at the origin of N. Moreover, metal-poor C-rich stars show variable s-process efficiencies, but s-process nucleosynthesis in AGBs at low metallicity is currently not well-constrained, and no clear explanation for this come from the models. Finally, some stars show r-process enhancement: this might be the trace of the contamination of the initial gas by a SNII of low energy (Umeda & Nomoto 2005), and, in these cases, is even an alternative scenario to the C-enrichment itself (see also alternative explanations, Goriely 2005, this volume). Due to the difficulty of the analysis of C-rich spectra, the number of high resolution studies is quite limited at the moment. Thus a more extensive analysis is required to better constrain nucleosynthesis at low $[\text{Fe}/\text{H}]$ and early chemical evolution.

References

- Alonso, A., Arribas, S., & Martínez-Roger, C. 1999, *A&AS*, 140, 261
 Alvarez, R., & Plez, B. 1998, *A&A* 330, 1109
 Arlandini, C., Käppeler, F., Wisshak, K., Gallino, R., Lugaro, M., Busso, M., & Straniero, O. 1999, *ApJ*, 525, 886
 Beers, T. C., Preston, G. W., & Shectman, S. A. 1992, *AJ*, 103, 1987
 Busso, M., Gallino, R., Lambert, D. L., Travaglio, C., & Smith, V. V. 2001, *ApJ*, 557, 802
 Cayrel, R., *et al.* 2004, *A&A*, 416, 1117
 Christlieb, N., Bessell, M. S., Beers, T. C., Gustafsson, B., Korn, A., Barklem, P. S., Karlsson, T., Mizuno-Wiedner, M., & Rossi, S. 2002, *Nature*, 419, 904
 Frebel, A., *et al.* 2005, *Nature*, 434, 871
 Goriely, S., & Siess, L. 2001, *A&A*, 378, L25
 Goriely, S., & Mowlavi, N. 2000, *A&A*, 362, 599
 Gustafsson, B., Bell, R. A., Eriksson, K., & Nordlund, A. 1975, *A&A*, 42, 407
 Gustafsson, B., Edvardsson, B., Eriksson, K., *et al.* 2003, in *stellar atmosphere modeling*, ASP Conf. 288, 331
 Hill, V., Plez, B., Cayrel, R., Beers, T. C., Nordström, B., Andersen, J., Spite, M., Spite, F., Barbuy, B., Bonifacio, P., Depagne, E., François, P., & Primas, F. 2002, *A&A*, 387, 560
 Keenan, P. C. 1942, *ApJ*, 96, 101
 Lucatello, Sara, PhD thesis, Dec. 2003
 McClure, R. D. & Woodsworth, A. W. 1990, *ApJ*, 352, 709
 Plez, B. 1992, *A&AS*, 94, 527
 Preston, G. W. & Sneden, C. 2001, *AJ*, 122, 1545
 Sneden, C., McWilliam, A., Preston, G. W., Cowan, J. J., Burris, D. L., & Armosky, B. J. 1996, *ApJ*, 467, 819
 Spite, M., *et al.* 2005, *A&A*, 430, 655
 Umeda, H., & Nomoto, K. 2005, *A&A*, 619, 427
 Van Eck, S., Goriely, S., Jorissen, A., & Plez, B. 2001, *Nature*, 412, 793
 Van Eck, S., Goriely, S., Jorissen, A., & Plez, B. 2003, *A&A*, 404, 291
 Wisotzki, L., Koehler, T., Groote, D., & Reimers, D. 1996, *A&AS*, 115, 227